



HAL
open science

Design of an Autonomous Ride-sharing Service through a Graph Embedding Integrated Dial-a-ride Problem: Application to the Last-mile Transit in Lyon City

Omar Rifki, Nicolas Chiabaut, Jean-Pierre Nicolas

► **To cite this version:**

Omar Rifki, Nicolas Chiabaut, Jean-Pierre Nicolas. Design of an Autonomous Ride-sharing Service through a Graph Embedding Integrated Dial-a-ride Problem: Application to the Last-mile Transit in Lyon City. Transportation Research Board (TRB) Annual Meeting 2021, Jan 2021, Virtual conference, United States. hal-04116307

HAL Id: hal-04116307

<https://hal.science/hal-04116307v1>

Submitted on 3 Jun 2023

HAL is a multi-disciplinary open access archive for the deposit and dissemination of scientific research documents, whether they are published or not. The documents may come from teaching and research institutions in France or abroad, or from public or private research centers.

L'archive ouverte pluridisciplinaire **HAL**, est destinée au dépôt et à la diffusion de documents scientifiques de niveau recherche, publiés ou non, émanant des établissements d'enseignement et de recherche français ou étrangers, des laboratoires publics ou privés.

1 **Design of an Autonomous Ride-sharing Service through a Graph Embedding Integrated**
2 **Dial-a-ride Problem: Application to the Last-mile Transit in Lyon City**

3

4

5 **Omar Rifki**

6 Univ. Lyon, École Urbaine de Lyon,

7 Univ. Gustave Eiffel, ENTPE, LICIT, UMR _T 9401 /

8 LAET, UMR 5593 CNRS, LYON, France.

9 Email: omar.rifki@gmail.com

10

11 **Nicolas Chiabaut**

12 Univ. Lyon, Univ. Gustave Eiffel, ENTPE, LICIT

13 UMR _T 9401, F-69518, LYON, France

14 Email: nicolas.chiabaut@entpe.fr

15

16 **Jean-Pierre Nicolas**

17 Univ. Lyon, ENTPE, LAET,

18 UMR 5593 CNRS, LYON, France.

19 Email: jeanpierre.nicolas@entpe.fr

20

21

22

23 Word Count : 7,210 words + 1 table (250 words per table) = 7,460 words

24

25

26

27

28

29 **AUTHOR CONTRIBUTIONS**

30 *The authors confirm contribution to the paper as follows: study conception and design: OR, NC, JPN;*

31 *data collection: OR; analysis and interpretation of results: OR, NC, JPN; draft manuscript preparation:*

32 *OR. All authors reviewed the results and approved the final version of the manuscript.*

1 **ABSTRACT**

2 Autonomous vehicles are anticipated to revolutionize ride-sharing services and subsequently enhance the
3 public transportation systems through a first-last mile transit service. Within this context, a fleet of
4 autonomous vehicles can be modeled as a Dial-a-Ride-Problem with certain features. In this study, we
5 propose a holistic solving approach for this problem, which combines the mixed-integer linear
6 programming formulation with a novel graph dimension reduction method based on the graph embedding
7 framework. This latter method is effective since accounting for heterogeneous travel demands of the
8 covered territory tends to increase the size of the routing graph drastically, thus rendering exact solving of
9 small instances computationally infeasible. An application is provided for the real transport demand of the
10 industrial district of “*Vallée de la Chimie*” in Lyon city, France. Instances involving more than 50
11 transport requests, and 10 vehicles could be easily solved. Results suggest that this method generates
12 routes of reduced nodes with a lower vehicle kilometers traveled compared to the constrained K-means
13 based reduction. Reductions in terms of GHG emissions are estimated to be around 75% lesser than the
14 private vehicle mode in our applied service. A sensitivity analysis is also provided.

15

16 **Keywords:** Shared Autonomous Mobility, First-Last Mile Service, Vehicle Routing, Node Embeddings.

1 **1. INTRODUCTION**

2

3 The urban expansion in most cities around the world followed an automobile-oriented pattern, leading to
4 the emergence of several low-density metropolitan areas, thus increasing the overall infrastructure costs
5 for public transportation (PT) (Sinha, 2003 [35]). Since then and due to this reason, PT systems have
6 been relegated to a secondary role behind private car use in urban mobility. The PT cover for low-density
7 areas and commercial and industrial districts outside the city is limited. Shared mobility, which is the
8 shared use of vehicles, bicycles, and other means of transport to access PT networks, started to appear to
9 be a viable solution to this issue, known as the first- and last-mile commute. The concept of shared
10 mobility is not novel in itself, and could be traced back to the 1990s where it was popular, and even to the
11 year of 1948 for the first car-sharing program (Shaheen & Chan, 2016 [36]). Yet, the major shift in shared
12 mobility is still expected by many to happen with the advent of shared autonomous vehicles (SAV).
13 Several AV manufacturers and service transportation provider companies have heavily invested and
14 adopted specific ride-sharing plans, e.g., Waymo in Phoenix area (Waymo, 2020 [41]), Jaguar Land
15 Rover (Jaguar Land Rover, 2020 [20]), and eventually Amazon, a fresh new competitor in this market
16 share (Amazon, 2020 [2]).

17

18 The factors making SAV an attractive transit mode are mainly economic, for both sides of customers and
19 PT and transportation network entities. Due to lower operational and investment costs over fixed routes,
20 transportation companies could propose services at fair prices with a higher frequency. Higher customer
21 satisfaction and time reductions may be equally obtained compared with other transit modes such as park-
22 and-ride and active modes. Another argument in favor of SAV lies in the environmental sustainability of
23 this technology, which is mainly due to the application of electric vehicles in SAV services. Autonomous
24 fleets could reduce GHG emissions by up to 73% compared to conventional taxi fleets (Bauer et al., 2018
25 [3]). It was shown that each SAV could replace around 11, respectively from 5 to 10 privately owned
26 vehicles, with an increase of 10%, resp. from 6 to 89% travel distance via agent-based simulations of the
27 city of Austin, Texas (Fagnant & Kockelman, 2014 [10]), resp. Lisbon (International Transport Forum,
28 2015 [19]). The existence of empty trips justifies this latter increase. All these favorable reports led to a
29 resurgence of small-size experimentations of SAV services in Europe, the U.S., and globally. Just in Lyon
30 city in France, where the case study of this paper is located, there are currently three experimentations:
31 Navya shuttle buses in the Confluence area, around Groupama stadium, and Mia buses in the Meyzieu-
32 Décine suburb area. Therefore, there is a great need of efficient design models for the short-time
33 deployment of SAVs, especially to handle the first-last mile transit issue (see Hyland & Mahmassani
34 (2017) [18] for a taxonomy of SAV fleet management problem classes to accompany this current mobility
35 shift).

36

37 A critical component of the design of an SAV service is the vehicle assignment or the process of
38 matching customer requests to vehicles. Most SAV approaches rely on rule-based assignment methods,
39 e.g., Gurumurthy & Kockelman (2018) [16]. Optimization models are almost not used here. This is
40 because SAV studies are mostly on-demand systems, that are dynamic systems that require solving
41 approaches that are computationally cost-efficient and easy to implement (Narayanan et al., 2020 [30]).
42 On the other hand, SAV models that are reservation-based, or in other terms static systems that could be
43 solved beforehand, are relying in general on optimization. However, they are quite few in number, e.g.,
44 Levin (2017) [22], Ma et al. (2017) [24]. Both Levin (2017) and Ma et al. (2017) proposed a linear
45 programming model to modelize an SAV fleet. In this study, we propose using the famous routing
46 problem of the Dial-a-Ride-Problem (DARP), which is derived from the classical Vehicle Routing
47 Problem (VRP) with additional constraints to account for pickup and drop-off requests. VRP and DARP
48 are both computationally intractable and can be pinned down as mixed-integer linear programming
49 models. According to Ho et al. (2018) [17], the largest instance solved to optimality for the basic DARP
50 with time windows is up to 8 vehicles and 96 requests, which is quite small for practical deployment of an
51 SAV service. Therefore, a mechanism has to be found in order to reduce the dimension of the routing

2

3

1 graph. To address this research gap, we develop a new reduction method based on the graph embedding
2 framework, specifically around the *node2vec* algorithmic framework (Grover and Leskovec, 2016 [14]),
3 which will be seen later. The problem we solve is a reservation-based SAV service.

4
5 A second objective is to design an SAV service as close as it would work in a real environment. First, this
6 was done by the choice of an application territory. We choose an industrial district in Lyon city (France),
7 called “Vallée de la Chimie” (VC). Although VC is one of the biggest chemical and petrochemical parks
8 in Europe, it is poorly served by public transport systems. It presents a concrete application of the last-
9 mile transit. This study focuses on a classical commute problem between the city center and suburbs
10 where two transportation alternatives compete: highway and rapid transit system. Second, we aim to
11 generate realistic traffic demand accounting for intermodality, i.e., using multiple transport modes on the
12 same trip. The traditional four-step travel models could only produce demand matrices for separate modes
13 (McNally, 2007 [26]). We have relied on a Land Use and Transport Interactions (LUTI) model-based tool
14 called OPTIREL to account for intermodality, without using agent-based simulations. OPTIREL has been
15 previously applied to design new subway lines in Paris among other projects. Therefore, the problem we
16 solve is tested on VC for the commute problem with a local rapid transit system.

17
18 The remainder of the paper is organized as follows. A brief literature review on the integration of PT-
19 SAV system, the DARP problem, and the graph embedding framework is presented in the next section.
20 Section 3 introduces the optimization model and the solving approach, while Section 4 describes the
21 study case and the generation of traffic demand. In Section 5, we experimentally evaluate the benefit of
22 the designed last-mile service, before concluding on some final thoughts.

23

24 **2. LITERATURE REVIEW**

25

26 In this section, we briefly review the literature of interest in this paper within the following three
27 subsections.

28

29 **Integration of PT-SAV systems**

30 Several recent studies are starting to explore the benefits of integrating SAV services with existing PT
31 systems. The most commonly adopted approach in this regard is agent-based simulations, whether it
32 concerns the integration, e.g., Shen et al. (2018) [37], Pinto et al. (2020) [31], or merely the intersection
33 of PT-SAV systems, e.g., Fagnant & Kockelman (2014) [10]. Liang et al. (2016) [23] proposed an
34 optimization model for an automated taxi service serving the last mile transit of a train system. Their
35 results are shown for a train station in Delft and include comparisons with human-driven taxis. Shen et al.
36 (2018) [37] simulate several scenarios of integrating bus lines with SAVs for the first-mile connectivity
37 during the morning peak hours. Their results based on the Singapore PT show significant savings if low-
38 demand buses are substituted by SAVs, savings that go up to 860 passenger car unit-kilometers. Pinto et
39 al. (2020) [31] proposed a bi-level optimization framework to simultaneously modelize the joint transit
40 network parameters and the SAV mobility service. The lower-level problem is a dynamic combined mode
41 choice – traveler assignment problem, while the upper-level is a modified transit network frequency
42 setting problem. Their results are given for the Chicago metropolitan area. A more detailed review of
43 overall SAV services is provided by Narayanan et al. (2020) [30].

44

45 **Dial-a-Ride problems**

46 Designing vehicle routes and schedules for collective people transportation such that each user request
47 has a pickup and a drop-off point locations are referred to as Dial-a-Ride systems, as in early versions of
48 this service, customers have to phone their requests. From a modeling perspective, DARP belongs to the
49 family of routing problems. It is a variant of the vehicle routing problem (VRP), precisely the capacitated
50 VRP with pickup and delivery and Time Windows, with a hands-on transporting passengers rather than
51 goods. Early solving approaches include Psaraftis (1980) [33], who solved the single-vehicle DARP using

1 dynamic programming, and Jaw et al. (1986) [21], who developed one of the first heuristics to the multi-
 2 vehicle DARP. For the exact approaches, Branch-and-Bound and their derived algorithms are the most
 3 applied, e.g., Ropke et al. (2007) [34], Gschwind & Irnich (2014) [15]. Concerning metaheuristics, those
 4 based on local search, especially those combining local search elements with other metaheuristics
 5 currently constitute state-of-the-art solvers, e.g. Masmoudi et al. (2016) [25]. Applications of DARPs are
 6 overall real-life problems with a diverse range of backgrounds, starting from the standard application to
 7 the elderly and disabled people transportation to health care services, to the current emerging applications
 8 in public transportation and shared mobility (Ho et al. 2018 [17], Mourad et al. 2019 [28]). For a more
 9 comprehensive review of the problem classes, solving algorithms, and the applications of the DARP, see
 10 Cordeau & Laporte (2007) [8], Molenbruch et al. (2017) [29], and Ho et al. (2018) [17].

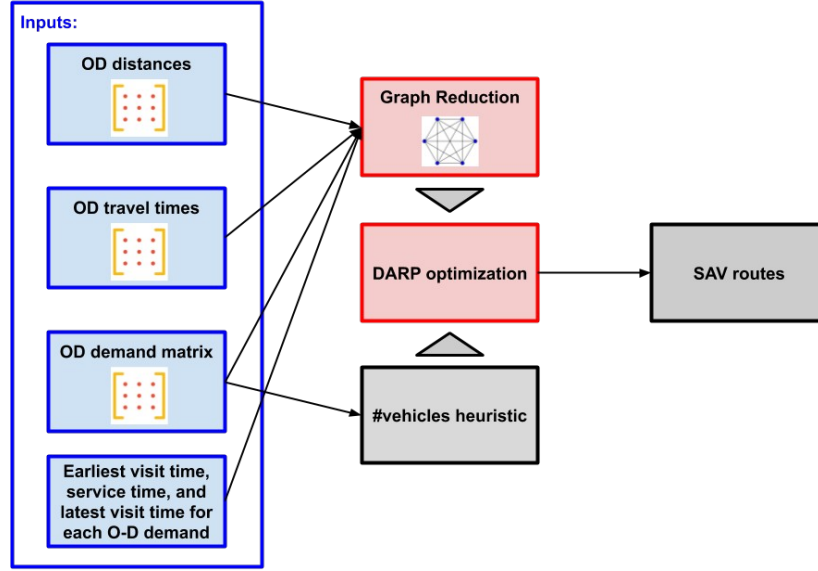
11 **Graph embeddings**

12 Graph embedding is a powerful method to represent a graph into a low-dimensional vector space by
 13 preserving as much as possible its topological structure. It addresses the research question of efficient
 14 graph analytics, since traditional methods suffer from the curse of dimensionality and space cost.
 15 Essential graph analytic tasks, such as graph classification, node clustering, and link prediction, become
 16 scalable to large instances. Representation learning and visualization is another research problem tackled
 17 by graph embeddings. There are three main categories of graph embeddings: probabilistic, matrix
 18 factorization-based, and deep learning-based methods (see Goyal & Ferrara, 2018 [13] for a survey on the
 19 topic). Probabilistic models learn the embedding of graphs through random walks. The samplings given
 20 by those walks can capture the neighborhood structure of nodes, connectivities, and other graph
 21 properties such as node centrality. Compared with other probabilistic models like *DeepWalk* (Perozzi et
 22 al., 2014 [32]) and *LINE* (Tang et al., 2015 [38]), the probabilistic model of *node2vec* (Grover &
 23 Leskovec, 2016 [14]) is shown to perform better. This is why we chose *node2vec* implementation for the
 24 graph embedding in the current study. The random walk exploration of this algorithm interpolates
 25 between breadth-first (BFS) and depth-first (DFS) searches in order to construct a more informative
 26 embedding.
 27

28 **3. PROPOSED METHOD**

29 Figure 1 illustrates the flowchart of the proposed approach. It is composed of two main distinct blocks:
 30 optimization according to the DARP formulation, and the graph reduction mechanism. Given a set of
 31 stations in the studied area, the method's inputs are the origin-destination (OD) matrix of the traffic
 32 demand, i.e., the number of customers traveling between any two stations, the duration of travel and the
 33 traveled distance between all couples of stations. The earliest visit time, service time, and latest visit time
 34 for each O-D couple of the demand matrix are also input data. Routing problems in their general
 35 formulation are defined on an underlying graph where the set of vertices corresponds to the depot and
 36 points to visit, and the set of arcs weighted with costs to travel, generally distances or travel times,
 37 represent shortest paths between stations. On this defined routing graph, each point has to be visited only
 38 once by precisely one vehicle. Since each initial station could be a pickup and a drop-off point to all the
 39 remaining stations, and taking into account all traffic demand inputs of the OD matrix of the area, the
 40 dimension of the routing graph to be solved can quickly increase. If n is the total number of stations, the
 41 graph dimension could attain a maximum of $n(n-1)$ points to visit without counting the depots. We
 42 assume that the vehicle's capacity is greater or equal to every entry of the OD demand matrix. This will
 43 prevent us from duplicating the same O-D couple of stations in the routing graph to account for the total
 44 demand. The graph reduction mechanism we propose aims to detect groups of pickup and drop-off couple
 45 points to be merged, and output a reduced graph that can be easily solvable by a mixed-integer
 46 programming solver. Note that clustering and community detection algorithms could be used as well in
 47
 48

1 the step of forming groups¹. We use the constrained K-means clustering method proposed Bradley et al.
 2 (2000) [5] for comparison matter. Our method is overall a model-based heuristic around a central
 3 component of mathematical programming. More details of the two main parts of our model is presented
 4 in the following.



5 **Figure 1. Flowchart showing the method's main modules.**

6
7
8 **Mathematical formulation**

9 In this study, we build on Cordeau (2006) [7] three-index formulation x_{ij}^k of the DARP by considering a
 10 new objective function and adding new variables. The points to visit are partitioned into two sets: the set
 11 of pickup points P and the set of drop-off points D , such that each demand request of the OD demand
 12 matrix has a pickup point $i \in P$, a corresponding delivery point which will be denoted $deliv(i) \in D$, a
 13 maximum riding time L_i , and a maximum waiting time M_i . Each point $i \in P \cup D$ has a service time ser_i
 14 , the earliest time to visit tw_i^{early} , a latest time to visit tw_i^{late} , and a demand load denoted req_i , such that for
 15 $i \in P, req_i \geq 0$ and $req_{deliv(i)} = -req_i$.

16
 17 K is the set of vehicles. Each vehicle $k \in K$ has a capacity $Q_k \in \mathbb{N}$, GHG emissions up to E_k by
 18 kilometer, starts from the depot denoted s_k and ends at the depot denoted e_k . Let $D_{start} = \{s_k : k \in K\}$ be
 19 the set of all start depots and $D_{end} = \{e_k : k \in K\}$ the set of all end depots. For all $j \in D_{start} \cup D_{end}$, the
 20 values $serv_j = req_j = 0$ are fixed. We associate different start and end depots to each vehicle to make the
 21 model more general. However, all these depots may correspond to the same geographical location, which
 22 coincide in the case of our application to the transit station of the PT network.

23
 24 The underlying routing graph $G = (V, A)$ has a vertex set equal to $V = P \cup D \cup D_{start} \cup D_{end}$. The arc
 25 set is defined as $A = \{(i, j) : (i \in D_{start}, j \in P) \vee (i \in D, j \in D_{end}) \vee (i, j \in P \cup D, i \neq j, i \neq deliv(j))\}$,

2 ¹ This is different from cluster and route methods, which first apply a clustering algorithm to the input visiting points, and
 3 second generate optimal routes for each cluster, e.g., Chen et al. (2020) [6].

1 and the weights of the graph are given by c_{ij} and d_{ij} , which denote respectively the duration to travel and
2 the distance from i to j .

3
4 The decision variable x_{ij}^k indicates whether the arc (i, j) is traversed by vehicle $k \in K$ or not, r_i and w_i
5 gives respectively the riding time and the waiting time for the request associated with pickup $i \in P$, t_i^k is
6 the arrival time at point i using vehicle k , and q_i^k is the load of the vehicle k when leaving the point i .

7
8 In addition to minimizing total travel times for all vehicles, the degree of customer dissatisfaction in the
9 sense of Psaraftis (1980) [33] is also minimized plus to the greenhouse gas emissions due to the transport
10 of passengers. Plausible values of E_k are drawn from the life-cycle assessment (LCA) conducted by
11 Gawron et al. (2019) [12]. $(\omega_1, \omega_2, \omega_3)$ gives the weights between the three quantities in the objective
12 function. The model is as follows.

$$15 \text{ Min } \omega_1 \sum_{k \in K} \sum_{i, j \in V} c_{ij} x_{ij}^k + \omega_2 \sum_{i \in P} (r_i + w_i) + \omega_3 \sum_{k \in K} \sum_{i \in V} \sum_{j \in V} E_k d_{ij} x_{ij}^k \quad (1)$$

16
17
18 Subject to:

$$19 \sum_{i \in P} x_{s_i}^k = \sum_{i \in D} x_{i_e}^k = 1 \quad (k \in K), \quad (2)$$

$$20 \sum_{k \in K} \sum_{j \in V} x_{ij}^k = 1 \quad (i \in P), \quad (3)$$

$$21 \sum_{j \in V} x_{ij}^k - \sum_{j \in V} x_{deliv(i)j}^k = 0 \quad (i \in P, k \in K), \quad (4)$$

$$22 \sum_{j \in V} x_{ji}^k - \sum_{j \in V} x_{ij}^k = 0 \quad (i \in P \cup D, k \in K), \quad (5)$$

$$23 t_j^k \geq (t_i^k + ser_i + c_{ij}) x_{ij}^k \quad (i, j \in V, k \in K), \quad (6)$$

$$24 t_{deliv(i)}^k \geq t_i^k + ser_i + c_{idiv(i)} \quad (i \in P, k \in K), \quad (7)$$

$$25 tw_i^{early} \leq t_i^k \leq tw_i^{late} \quad (i \in P \cup D, k \in K), \quad (8)$$

$$26 q_j^k \geq (q_i^k + req_i) x_{ij}^k \quad (i, j \in V, k \in K), \quad (9)$$

$$27 r_i \geq t_{deliv(i)}^k - (t_i^k + ser_i) \quad (i \in P, k \in K), \quad (10)$$

$$28 w_i \geq t_i^k - tw_i^{early} \quad (i \in P, k \in K), \quad (11)$$

$$29 c_{idiv(i)} \leq r_i \leq L_i \quad (i \in P), \quad (12)$$

$$30 0 \leq w_i \leq M_i \quad (i \in P), \quad (13)$$

$$31 0 \leq q_i^k \leq Q_k \quad (i \in V, k \in K), \quad (14)$$

$$32 x_{ij}^k = 0 \vee 1 \quad (i, j \in V, k \in K). \quad (15)$$

33
34 The routing constraints (2)-(5) ensure that each vehicle starts and ends at its corresponding depot points in
35 constraint (2), each request is answered in constraint (3), the same vehicle is used for pickup and drop-off
36 in constraint (4), and the flow conservation in constraint (5). Constraint (6) tracks the service time, while
37 constraint (7) ensures that pickup points are visited before their delivery points, and time window
38 constraints are given in (8). Constraint (9) tracks the load of vehicles, which is needed later to compute
39 the vehicle occupancy rate (VOR) indicator. Constraints (10) and (11) are respectively relative to the
40 riding time and the waiting time for each request. Constraints (12)-(15) represent the binary and the
41 bounding restrictions for the decision variables. Note that the current mixed-integer programming solvers

1 can efficiently handle indicator constraints as in (6) and (9). Other useful constraints to add concern the
 2 battery management aspect, which includes the recharge time, the battery energy consumption and
 3 detours to recharge stations as in Bongiovanni et al. (2019) [4]. Recent simulations (Vosooghi et al., 2020
 4 [40]) suggest that a best strategy for SAV could be deploying batteries with more charging space to avoid
 5 charging the battery within the rush hours of the morning and the evening peaks, otherwise alternating
 6 charging and routing could drastically increase the passenger kilometer traveled. For this reason and for
 7 the time being, we suppose that battery charging operations are set outside the routing process, and that
 8 vehicles are set to be initially charged before transporting customers.

9
 10 For the heuristic to determine the number of vehicles $|K|$ (mentioned in Figure 1), we use the following
 11 formula for vehicles with an identical capacity $Q=Q_k$:

$$12 \quad \text{vehicles}(m) = \sum_{i,j \in V^2, i \neq j} \text{demand}(i,j) / (n \times Q).$$

13
 14 m is an estimate of the average number of O-D requests each vehicle is expected to answer during the
 15 time horizon (usually $m=3$ or 4).
 16
 17
 18

19 **Graph reduction mechanism**

20 The steps of the graph reduction are listed in the below algorithm. At first, *node2vec* is applied to the
 21 routing graph G , which is introduced in the previous section and is weighted by the travel durations
 22 $(c_{ij})_{i,j \in A}$, for the following inputs: the desired dimension size of the embedding d , the number of random
 23 walks to launch from each node and their length, plus other parameters related to the guided exploration
 24 strategy of the walks. Thereafter, each node of G can be represented by a feature vector of dimension d .
 25 To obtain a similarity matrix S for the nodes of G , we apply the cosine similarity, which is defined for
 26 any two real-valued vectors v_1 and v_2 as the cosine of the angle θ between them, i.e.,
 27 $\cos(\theta) = v_1 \cdot v_2 / (\|v_1\| \times \|v_2\|)$. Other measures of similarity and distances could be also used at this step.
 28 This step is important because it gives a quantification of the similarity between any two nodes of G
 29 while taking into account as much as possible the topology structure of the graph.
 30

31 The remaining steps concern merging the points to visit. We opt for merging pick-up and drop-off (P-D)
 32 couples two by two. This gives us more flexibility in the rate of contraction of the graph G , and allows us
 33 to quickly compute the optimal order within the merged P-D couples. For each two P-D couples
 34 $(p_1, \text{deliv}(p_1), p_2, \text{deliv}(p_2))$, we compute the following average similarity using the similarity matrix S

$$35 \quad \text{simil}(p_1, p_2) = \left(S(p_1, p_2) + S(\text{deliv}(p_1), \text{deliv}(p_2)) + S(p_1, \text{deliv}(p_1)) \right) / 6 \\
 36 \quad + \left(S(p_2, \text{deliv}(p_2)) + S(p_2, \text{deliv}(p_1)) + S(p_1, \text{deliv}(p_2)) \right) / 6, \quad (17)$$

37
 38 which indicates how close the two couples are. Note that we affect a higher input parameters for BFS
 39 over DFS in the guided search of *node2vec* to favor closer nodes within the vicinity of each node of G .
 40 After ranking pairs of the P-D couples by their similarity, we choose the top $r \times (|P| \cup |D|) / 2$ pairs, with
 41 r is the rate of contraction of the graph. The following step proceeds by computing the optimal order of
 42 visiting points within each of the chosen pairs. There are only six possible orders respecting the pickup
 43 and drop-off constraints among the total 32, which are shown in Figure 2-a. For each optimal order, we
 44 output two aggregated nodes in the novel graph, i.e., if an optimal order is for instance
 45 $(p_1, \text{deliv}(p_1), p_2, \text{deliv}(p_2))$, the new nodes will correspond to $p' = (p_1, \text{deliv}(p_1))$ and

1 $deliv(p') = (p_2, deliv(p_2))$. The final step updates the graph weights involving the new nodes, as shown
 2 in Figure 2-b. Distances between nodes are updated in the same manner. The graph reduction algorithm
 3 has an overall time complexity of $O(|V|^2)$, since *node2vec* runs in $O(|V|^2)$ and the number of pairs of P-
 4 D couples processed in the merging steps is at maximum $COMBIN(n = (|P| \cup |D|)/2, k=2) \leq |V|^2/8$.

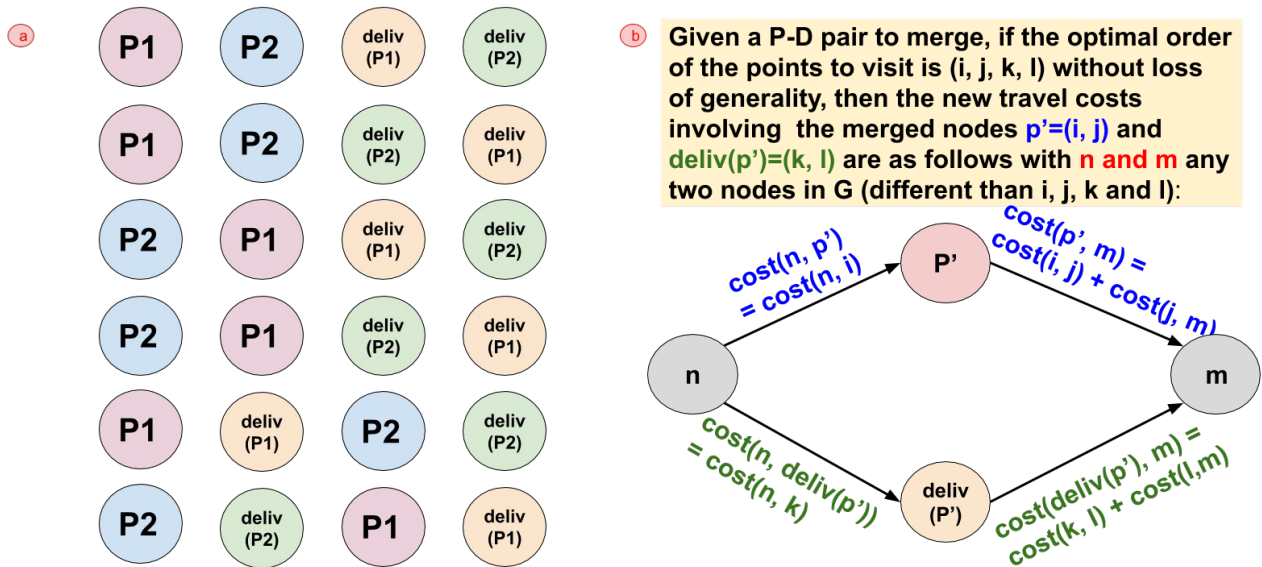
5
6

Algorithm: *node2vec*-based graph reduction

Inputs: The routing graph $G=(V, A)$, the contraction rate r .

1. Apply the *node2vec* algorithm to G .
 2. Compute the similarity matrix S of G using the cosine measure on the embedding of 1.
 3. Compute for each two P-D couples $(p_1, deliv(p_1), p_2, deliv(p_2))$ the value $simil(p_1, p_2)$.
 4. Select the top $r \times (|P| \cup |D|)/2$ similar pairs of P-D couples.
 5. Compute the optimal order of points to visit within each chosen pair.
 6. Update the graph's costs for the arcs going to/coming from the newly merged nodes.
-

7
8
9
10



12 **Figure 2. Possible arrangements for a pair of P-D couples in (a),**
 13 **and the updated travel costs involving merged P-D pairs in (b).**
 14

1 **4. CASE STUDY: THE INDUSTRIAL DISTRICT OF “VALLÉE DE LA CHIMIE”, LYON CITY**

2
3 In this section, we describe the studied territory and the process used to generate the input demand data.

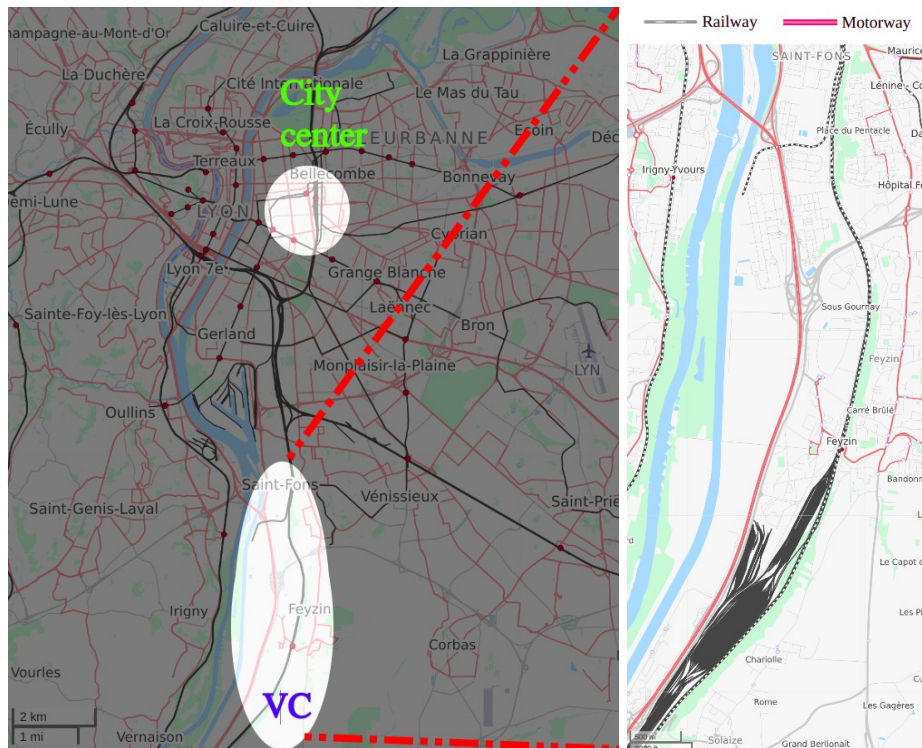
4
5 **Territory**

6 Lyon is the second-largest urban area of France and is home to several industrial hubs. The largest of
7 them is “Vallée de la Chimie” (VC) for approximately 17 km^2 . Situated about 10 km away from city
8 center, VC has currently over 1,000 companies, 6 research and development centers, mostly working in
9 the chemical, energy and the environmental sectors, and it attracts over 20,000 jobs (Métropole de Lyon,
10 2020 [27]).

11
12 In terms of mobility infrastructure, a Rapid Transit System (RTS) links VC to the city center on a regular
13 schedule (each 30 min in rush hours, otherwise once by hour). There are quite few buses connecting VC
14 to Lyon city (in total three, two are drawn in the right map of Figure 3 in light red lines). The highway A7
15 also crosses the territory. This artery is essential for logistic transportation and gets severely congested in
16 the morning rush hours, as A7 is also the south entry point to the city. Commuting to work accounts for a
17 significant part of mobility flows from/to VC. By considering the low PT supply and the highway’s high
18 saturation, a typical last-mile transit issue occurs. A number of experimentations to overcome this issue
19 are currently conducted in this territory: Personal Rapid Transit (PRT) from the Esprit project (Esprit,
20 2019 [9]) and a demand-responsive transit (DRT) service from the local PT service (TCL, 2020 [39]). VC
21 constitutes a good study example for the SAV deployment.

22
23 This test case is finally classic and generalizable to several other mobility situations all over the world.
24 Indeed, it corresponds to the framework of a commute problem with two main alternatives: PT and the
25 private vehicle which experiments bottleneck.

26

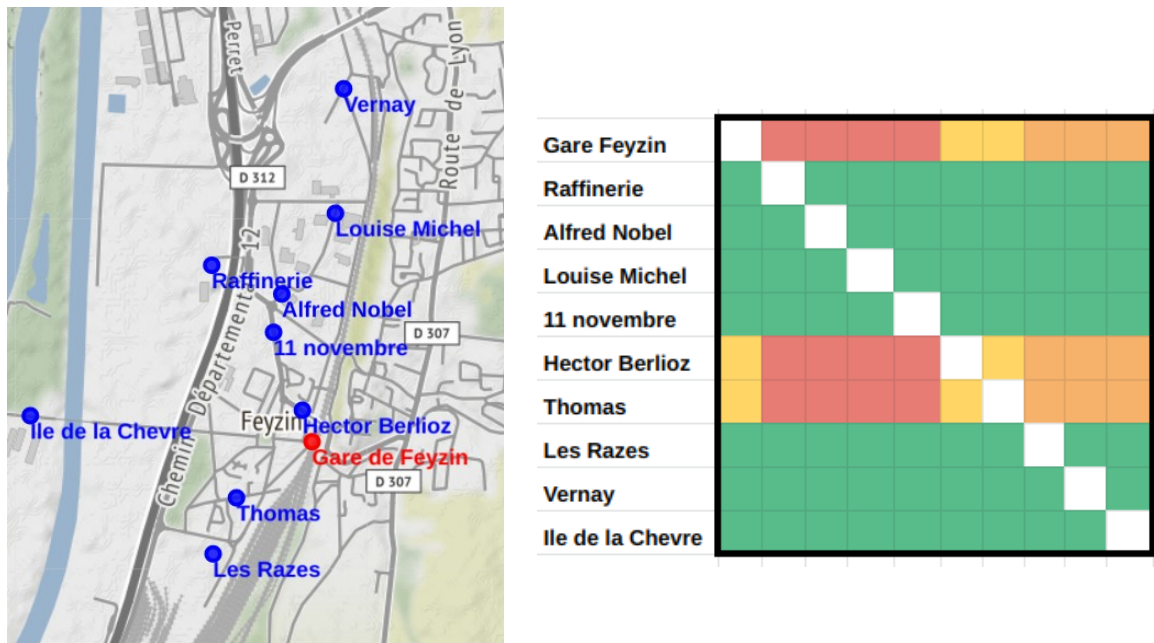


27 **Figure 3. The placement of VC within the Lyon urban area in the left map, and**
28 **the transport network connecting VC in the right map. Source: www.openstreetmap.org/.**

1 **Demand generation**

2 To generate the traffic demand, we apply a Land Use and Transport Interaction (LUTI) model. LUTI
 3 models are spatial interaction models that integrate the socio-demographic and economic features of the
 4 population to the transport infrastructure and mobility features, to answer questions such as, what is the
 5 transport modal share of a middle-sized income household living in the suburb to commute to work to the
 6 city center. With LUTI models, the cause/effect relationships between land use and transport become well
 7 understood, and the mobility patterns are well identified. It is noteworthy that LUTI models are
 8 extensively used for urban and transport plannings (see Acheampong et al., 2015 [1] for a review on the
 9 topic).

10
 11 We use the LUTI model called OPTIREL, which has the advantage to account for intermodality.
 12 OPTIREL proceeds by decomposing the area’s space according to the transport mode used from/to the
 13 target territory. For instance, the first zone of the studied territory is solely accessible by walking, the
 14 second zone is larger and is accessible by bus or RTS system (from/to the territory), the third zone is even
 15 larger. It delimits areas accessible by private vehicles combined with relay parking. In this manner, it is
 16 possible to define mobility solutions combining several modes in the step of the modal decomposition.
 17 The classical four-step travel models define zones according to the administrative or the population
 18 census based spatial decomposition, which turns out to be a rigid assumption for combining several
 19 modes in the third step of modal share. The traffic demand considered in our application corresponds to
 20 the PT demand arriving in the territory by train during the morning peak [7h-10h]. This interval will set
 21 our time horizon. Ten stations are defined for the planned SAV service, which correspond to stations of
 22 the Esprit project (Esprit, 2019 [9]), and cover the north part of VC. They are shown in Figure 4. The
 23 main transit station is “Gare Feyzin” which will coincide with the depots of all vehicles. We can notice
 24 from our input OD demand matrix, generated by OPTIREL, and shown in Figure 4, that traffic coming
 25 from “Gare Feyzin” is the highest. Interestingly, the traffic is also high from the stations “Hector
 26 Berlioz” and “Thomas” which are the closest stations to the transit station. Finally, duration and distances
 27 between stations are generated using web mapping services.



49 **Figure 4. The locations of the ten stations considered in the study (left map), and the input OD**
 50 **demand matrix (right plot), which is colored according to the demand intensity: green=low, yellow**
 51 **and orange=middle, and red=high.**

1 **5. RESULTS**

2

3 In this section, we test the proposed method on the study case and show its usefulness.

4

5 **Parameters setting**

6 For solving the DARP, ILOG CPLEX 12.10 solver is used, with the termination criteria set to a relative
 7 gap of 1%. Although the routing graph is reduced, we have noticed that the problem (1)-(15) takes
 8 extended time to find a first solution, which is not the case for the problem (1)-(15) excluding the
 9 precedence constraint (7). Thus, we solve the latter problem in a first step, rearrange the points to visit
 10 for each vehicle by solving the single-vehicle DARP problem (1)-(15), and then consider this solution a
 11 starting point for our main optimization. The effect of adding an initial good quality starting point is
 12 beneficial in our CPLEX solving process. In the absence of precise data about the customers' time
 13 windows, we set the constraints (8) to two time windows, each with one hour duration, and uniformly at
 14 random partition P and D points on the two time windows, with the condition that each dropoff point has
 15 the same time window of its pickup point. We do not consider customers waiting times w_i with this
 16 configuration of time windows. A fixed service time $ser_i=1$ minute is associated to each point to visit
 17 $i \in P \cup D$. In the baseline scenario, we set the capacity of vehicles to
 18 $Q=25 > 20 = \max_{i,j \in V^2, i \neq j} demand(i,j)$, the number of vehicles to $vehicles(m=3)=4$, the maximum
 19 riding time to $L=15$ minutes, and the weights of the objective function to $(\omega_1, \omega_2, \omega_3)=(1,1,0.1)$. The
 20 GHG emission rate is chosen to be equal to $E_k=0.171 \text{ Kg CO}_2 - eq/km$, which corresponds to the short-
 21 range electric autonomous taxi scenarios in Gawron et al. (2019) [12]. For the input parameters of
 22 $node2vec$, the dimension size is set to 30, while the walk length is equal to 6 for 1000 random walks
 23 launched from each node. Since $node2vec$ is a stochastic method, we launch this method multiple times,
 24 exactly 50 times for each configuration of Q and L , then choose the instance with the minimal inside
 25 travel time. This latter value is given by the summation of travel times inside the reduced nodes. For
 26 instance, the inside travel time of the graph of Figure 2-b is equal to $c_{ij}+c_{kl}$. The calculation is done for
 27 each configuration of Q and L as the possible arrangements of P-D couples could be less than six (Figure
 28 2-a). All experiments are performed on an Intel(R) Core(TM) i7-8750H CPU @ 2.20GHz machine with
 29 32 GB RAM memory.

30

31

32 **Constrained K-means**

33 The constrained K-means clustering proposed by Bradley et al. (2000) [5] extends the traditional
 34 algorithm ensuring that each cluster contains at least a minimum number of elements. The problem of
 35 minimum cost flow optimization is used to solve the new formulation. Similarly, it is possible to add a
 36 maximum size constraint to clusters. In order to have a fair comparison with $node2vec$, we associate to
 37 each pickup node a value similar to the average of the expression (17) :

38

$$39 \quad cost_{avg}(p) = \sum \left(c_{pq} + c_{deliv(p)deliv(q)} + c_{pdeliv(p)} + c_{qdeliv(q)} + c_{pdeliv(q)} + c_{qdeliv(p)} \right) / 12$$

$$40 \quad + \sum \left(c_{qp} + c_{deliv(q)deliv(p)} + c_{deliv(p)p} + c_{deliv(q)q} + c_{deliv(q)p} + c_{deliv(p)q} \right) / 12.$$

41

42 This expression has twelve terms for each $q \in P$ to account for the asymmetry of the travel times c_{ij} .
 43 Clusters are generated with a maximum size of two and a minimum size of one, for the clustering with the
 44 best inside travel time among 50 runs.

45

46

47

48

1 **Indicators**

2 Two main performance measures are used: the vehicle kilometers traveled (VKT), and the vehicle
 3 occupancy rate (VOR). Two additional measures are extracted from them. VKT indicates the total
 4 distance traveled by all vehicles of K to satisfy the demand, and is equal to,

$$5 \quad VKT(x) = \sum_{k \in K} \sum_{i, j \in V^2, i \neq j} d_{ij} x_{i,j}^k.$$

6 We also use a correlated measure to VKT, which is the total GHG emissions generated for all trips to
 7 provide an order of magnitude of SAV emissions : $GHG(x) = E_k VKT(x)$. To get a glimpse of the GHG
 8 environmental gain of using SAV, which is previously established in the literature, we show the gap:

$$9 \quad GHG_{gain}(x) = \frac{GHG_{pv}(demand) - GHG(x)}{GHG_{pv}(demand)},$$

10 with $GHG_{pv}(demand)$ represents GHG emissions estimated for the input demand and the personal
 11 vehicle mode.

12

13 The third measure VOR is an average of the load rate of all vehicles at each step of the routing, and is
 14 equal to,

$$15 \quad VOR(x, q) = \frac{1}{|K|} \frac{1}{|P| \cup |D|} \sum_{k \in K} \sum_{i, j \in P \cup D, i \neq j} x_{ji}^k \frac{q_i^k}{Q}.$$

16 VOR can also be seen as an index of comfort of the mobility service. The last measure, the zero
 17 occupancy rate (ZOR) is equal to the percentage of trips between any two stations which have an
 18 occupancy rate equal to zero, and is given by,

$$19 \quad ZOR(x, q) = \frac{1}{|K|} \sum_{k \in K} \sum_{i, j \in P \cup D, i \neq j, q_i^k = 0} \frac{x_{ji}^k}{(|P| \cup |D|) - 1}.$$

20 All measures are computed on the original non-reduced problem.

21

22

23 **Baseline scenario**

24 Accounting for the total demand of VC leads to solving a problem of 54 points to visit² plus the dummy
 25 start and end vehicle depots, which is a computationally hard problem for $k > 2$ vehicles. The graph
 26 reduction mechanism makes this optimization more manageable. CPLEX solver could attain a solution
 27 for the baseline scenario within a relative MIP gap of 23% in 0.28, 277.17, and 3609.62 seconds when the
 28 graph contraction rate is respectively 50%, 45%, and 40%. In the rest of the study, we set the contraction
 29 rate of the routing graph at $r = 50\%$. Figure 5 illustrates the SAV routes obtained for the baseline
 30 scenario. This scenario has a total traveled distance of $VKT = 65.46$ (respectively $74.44 km$) for an
 31 average occupation rate of $VOR = 42.1\%$ (resp. 31.6%), and a total emissions of $GHG = 11.12$ (resp.
 32 $12.73 Kg CO_2 - eq$) for *node2vec* (resp. constrained K-means) based node reduction. By drawing on the
 33 estimates of the vehicle occupancy rate and the GHG emissions of private vehicles computed for the
 34 Lyon urban area (François et al, 2017 [11]), we obtain :

$$35 \quad GHG_{pv}(demand) = \sum_{i, j \in V^2, i \neq j} demand(i, j) \times d_{ij} \frac{175 g CO_2 - eq / Km}{1.33 person / car} = 43.8 Kg CO_2 - eq.$$

36 Therefore, compared to the private vehicle mode, the SAV service leads to a reduction of 74.61% of
 37 GHG emissions for the territory of VC when relying on the *node2vec* reduction.

38

39

2 The number of points to visit for the full OD demand matrix of Figure 4 is 180 points. We have only 54 points in our input
 3 data, since some O-D couples have a null demand.

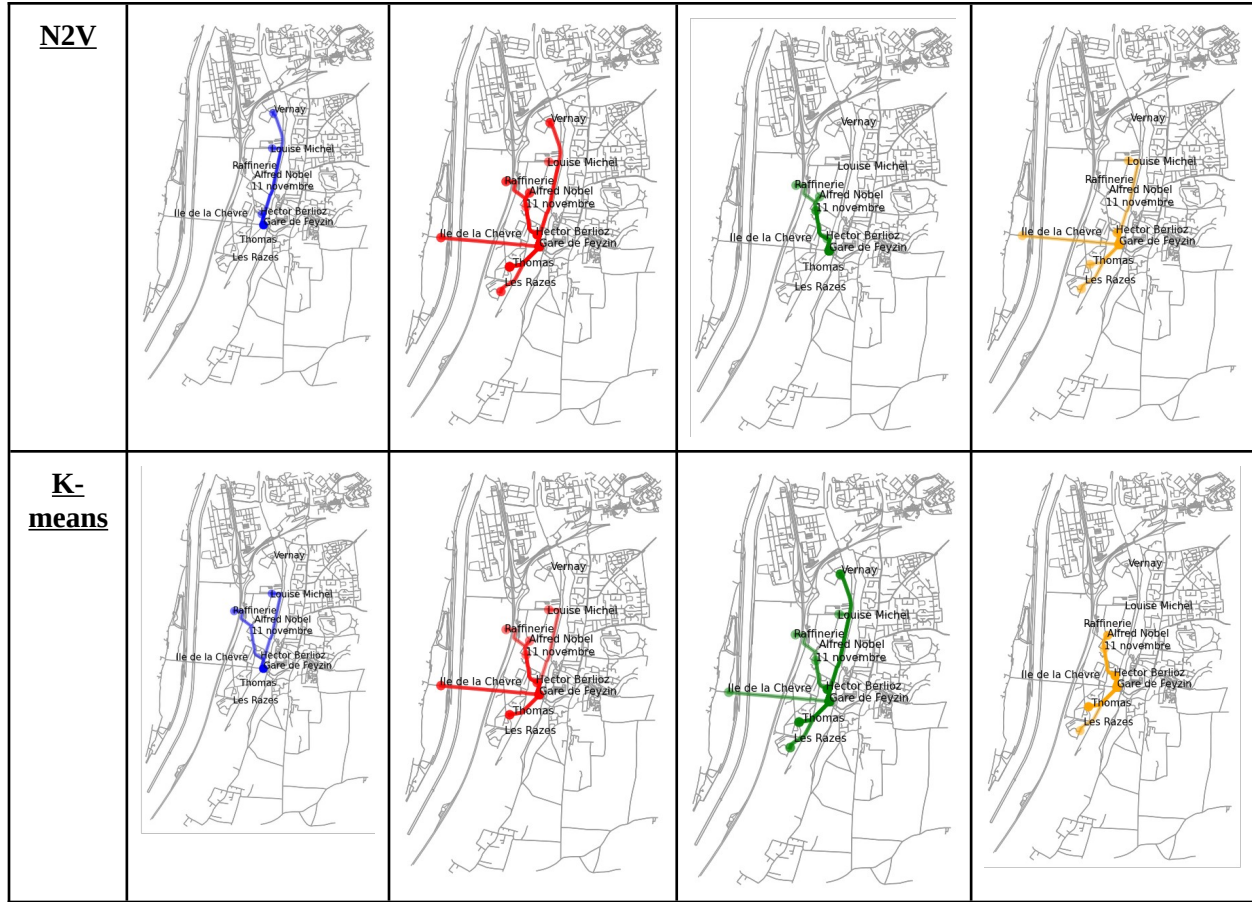


Figure 5. SAV routes for the baseline scenario with the graph embedding reduction (first row) and the K-means based reduction (second row).

1
2
3
4
5
6

Sensitivity analysis

7 Figure 6 shows the sensitivity analysis performed on the baseline scenario, by varying the fleet size $|K|$,
 8 the maximum riding time L , and the vehicle’s capacity Q . For a number of vehicles equal to 1, 5, and 10,
 9 the total traveled distance VKT slowly decreases to be resp. 67.70, 64.53, and 59.88 km for the *node2vec*
 10 reduction. K-means clustering generates tours in the same decreasing trend, but with higher VKT, which
 11 is an indication of a lower performance to find best pairs of P-D couples to merge. While $|K|$ is
 12 multiplied by 10, VKT of *node2vec* is divided by 1.13. Having more vehicles actually allows more
 13 flexibility for the routing optimization to produce efficient assignments of vehicles to the transport
 14 requests. VKT is decreasing in function of Q , which is expected since larger capacities imply smaller
 15 tours. *Node2vec* is again much efficient than K-means reduction in this regard. VKT is overall stable
 16 under varying L . As some values of L and Q may constraint the number of possible arrangements of
 17 Figure 2-a, an oscillatory effect when varying L and Q could be seen for VKT and VOR index as well.
 18 GHG_{gain} plots on the other hand show the substantial cut in terms of GHG emissions if SAV are deployed
 19 instead of private vehicles, especially for the *node2vec* method. The reduction corresponds to resp.
 20 73.57% and 76.62% of GHG emissions if the fleet size is equal to resp. 1 and 10. Concerning the vehicle
 21 occupation rate, we notice that this rate is not affected much by the size $|K|$ and the riding time L , and
 22 oscillates around the mean value of 35%. The vehicle’s capacity Q , on the other hand, has some influence
 23 on VOR. VOR decreases from 38.5 (resp. 43.3%) to 24.9 (resp. 22.7%) when the capacity increases from

2
3

1 20 to 50 for *node2vec* (resp. K-means) reduction. This particular point should be carefully considered by
2 the designers of SAV services to achieve a fair tradeoff between users' comfort and the costs for an
3 additional capacity of automated vehicles and buses. As for empty trips, ZOR is solely impacted by the
4 size $|K|$. This index decreases for an increase of $|K|$, otherwise it has a constant value around 10%.

5
6

7 **6. CONCLUSION**

8

9 In this study, we propose a model-based heuristic design for a shared autonomous vehicle (SAV) service
10 by combining the formulation of the Dial-a-Ride-Problem (DARP) and a graph reduction mechanism.
11 This latter procedure is based on the graph embedding framework *node2vec*, and allows us to merge
12 similar couples of pickup and drop-off points, and hence solving instances with a large number of O-D
13 requests and fleet size. A study case analysis is provided for an industrial district of the Lyon urban area
14 (France), wherein the traffic demand is generated by a LUTI model. In the paper, we address in a classical
15 commute problem between city center and suburbs where two transportation alternatives compete:
16 highway and rapid transit system (RTS). The SAV service is deployed as a last-mile transit for the RTS.
17 Our results suggest that *node2vec* is more efficient for node reduction than the constrained K-means (in
18 terms of vehicle traveled distance), in addition around 75% reduction of GHG emissions are gained by
19 SAV service when compared to the private vehicle choice.

20

21 The limitations of the study mainly concerns the maximum reduction rate, which is currently 50% as
22 reduction is done by merging couples of pickup and drop-off pairs, and the specificity of our application
23 case. One natural improvement is to enlarge the reduction mechanism to three pickup and drop-off pairs.
24 We also think that integrating the current approach with the LUTI model would generate precise
25 partitions of the mode share for the studied territory and population, which would in return help to fix the
26 adequate parameters of the SAV service, i.e., load capacity, fleet size, maximum riding time, in a cause-
27 and-effect loop.

28

29

30 **ACKNOWLEDGEMENTS**

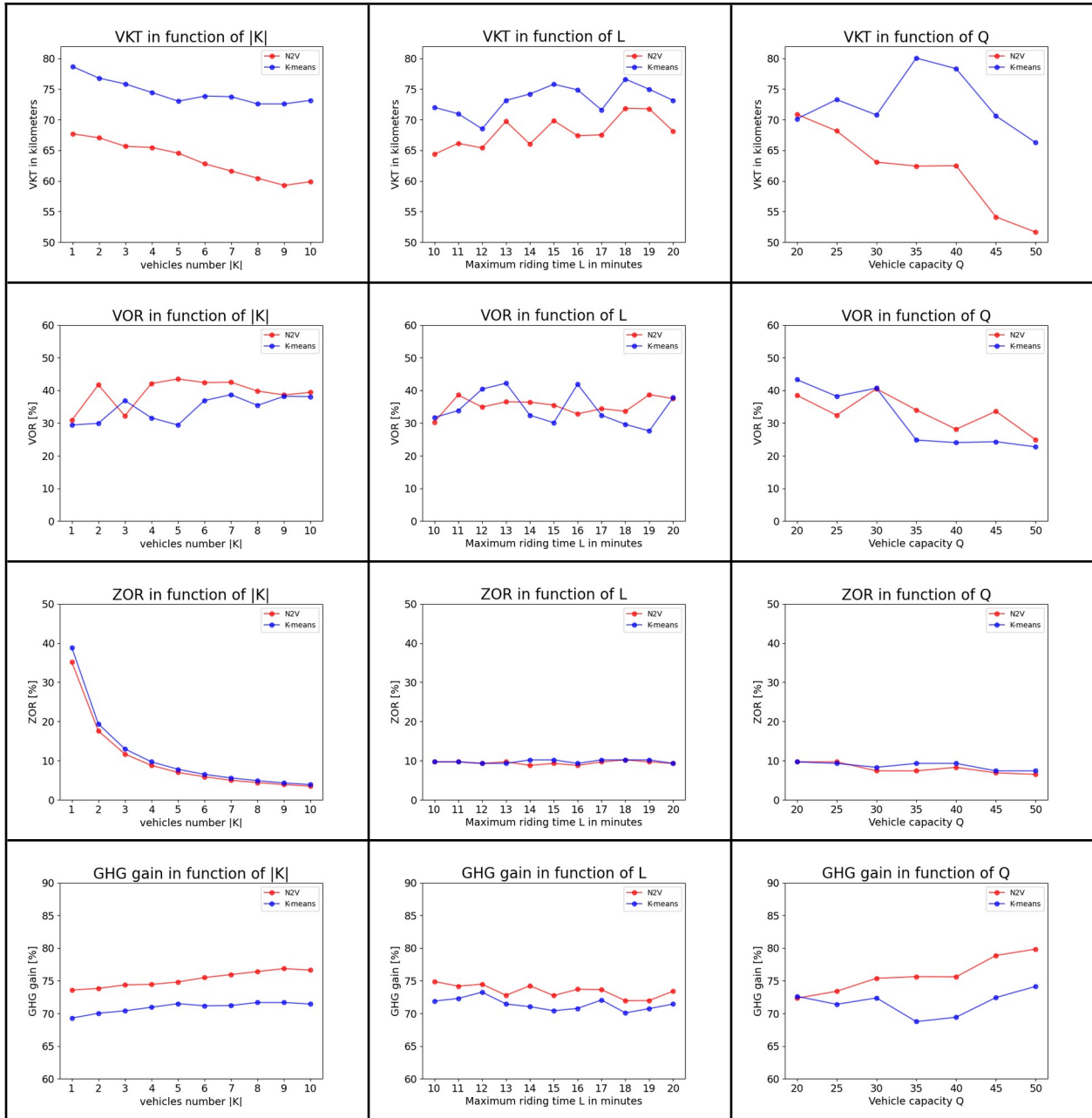
31 This work is supported by "Lyon Urban School" (ANR-17-CONV-0004) of Université de Lyon, within
32 the program "Investissements d'Avenir" (ANR-11-IDEX-0007) operated by the French National
33 Research Agency (ANR). We would like to warmly thank Guy Bourgeois for making the data of
34 OPTIREL available.

35

36

37

1



2
3
4
5
6
7

Figure 6. Sensitivity analysis on the baseline scenario of the fleet size (first column), the clients maximum riding time (second column) and the vehicles' capacity (third column) for the indicators VKT (fist row), VOR (second row), ZOR (third row) and GHG gain (fourth row).

2
3

Table 1. Numerical values of the sensitivity analysis (plotted in Figure 6).

Fixed parameters	Variable parameter	VKT [Km]		VOR [%]		ZOR [%]		GHG [Kg CO2-eq]	
		N2V	K-means	N2V	K-means	N2V	K-means	N2V	K-means
Q = 25 L = 15 min	K = 1	67.7	78.7	30.8	29.4	35.2	38.9	11.6	13.45
	K = 2	67.0	76.8	41.7	29.9	17.6	19.4	11.5	13.13
	K = 3	65.6	75.8	32.2	36.9	11.7	13.0	11.2	12.97
	K = 4	65.5	74.4	42.1	31.6	8.8	9.7	11.2	12.73
	K = 5	64.5	73.0	43.5	29.4	7.0	7.8	11.0	12.49
	K = 6	62.8	73.9	42.4	36.9	5.9	6.5	10.7	12.63
	K = 7	61.6	73.7	42.5	38.7	5.0	5.6	10.5	12.61
	K = 8	60.4	72.6	39.8	35.4	4.4	4.9	10.3	12.41
	K = 9	59.3	72.6	38.6	38.2	3.9	4.3	10.1	12.41
	K = 10	59.9	73.2	39.4	38.1	3.5	3.9	10.2	12.51
K = 4 Q = 25	L = 10min	64.3	72.0	30.3	31.7	9.7	9.7	11.0	12.31
	L = 11min	66.1	70.9	38.6	33.8	9.7	9.7	11.3	12.1
	L = 12min	65.4	68.5	34.9	40.4	9.3	9.3	11.2	11.7
	L = 13min	69.7	73.2	36.5	42.2	9.7	9.3	11.9	12.5
	L = 14min	66.0	74.2	36.4	32.4	8.8	10.2	11.3	12.7
	L = 15min	69.8	75.8	35.5	30.1	9.3	10.2	11.9	13.0
	L = 16min	67.4	74.9	32.8	41.9	8.8	9.3	11.5	12.8
	L = 17min	67.5	71.6	34.4	32.4	9.7	10.2	11.5	12.2
	L = 18min	71.9	76.6	33.6	29.6	10.2	10.2	12.3	13.1
	L = 19min	71.8	74.9	38.7	27.6	9.7	10.2	12.3	12.8
L = 20min	68.1	73.2	37.5	37.8	9.3	9.3	11.6	12.5	
K = 4 L = 15 min	Q = 20	70.9	70.1	38.5	43.3	9.7	9.7	12.1	11.0
	Q = 25	68.2	73.3	32.4	38.2	9.7	9.3	11.7	12.5
	Q = 30	63.1	70.8	40.5	40.7	7.4	8.3	10.8	12.1
	Q = 35	62.4	80.1	34.0	24.8	7.4	9.3	10.7	13.7
	Q = 40	62.5	78.3	28.1	24.0	8.3	9.3	10.7	13.4
	Q = 45	54.1	70.6	33.6	24.3	6.9	7.4	9.3	12.1
	Q = 50	51.6	66.2	24.9	22.7	6.5	7.4	8.8	11.3

1 **REFERENCES**

- 2 1. Acheampong RA, Silva EA. Land use–transport interaction modeling: A review of the literature and
3 future research directions. *Journal of Transport and Land use*. 2015 Jan 1;8(3):11-38.
4
5 2. Amazon. Article titled “Amazon Buys Autonomous Taxi Company Zoox. Look Out, Uber and Lyft.”,
6 by Eric J. Savitz. 2020, June 26. URL: [https://www.barrons.com/articles/amazon-buys-autonomous-taxi-](https://www.barrons.com/articles/amazon-buys-autonomous-taxi-company-zoox-51593187053)
7 [company-zoox-51593187053](https://www.barrons.com/articles/amazon-buys-autonomous-taxi-company-zoox-51593187053) [accessed July 20, 2020].
8
9 3. Bauer GS, Greenblatt JB, Gerke BF. Cost, energy, and environmental impact of automated electric taxi
10 fleets in Manhattan. *Environmental science & technology*. 2018 Mar 28;52(8):4920-8.
11
12 4. Bongiovanni C, Kaspi M, Geroliminis N. The electric autonomous dial-a-ride problem. *Transportation*
13 *Research Part B: Methodological*. 2019 Apr 1;122:436-56.
14
15 5. Bradley PS, Bennett KP, Demiriz A. Constrained k-means clustering. Microsoft Research, Redmond.
16 2000 May;20(0):0.
17
18 6. Chen S, Wang H, Meng Q. Solving the first-mile ridesharing problem using autonomous vehicles.
19 *Computer-Aided Civil and Infrastructure Engineering*. 2020 Jan;35(1):45-60.
20
21 7. Cordeau JF. A branch-and-cut algorithm for the dial-a-ride problem. *Operations Research*. 2006
22 Jun;54(3):573-86.
23
24 8. Cordeau JF, Laporte G. The dial-a-ride problem: models and algorithms. *Annals of operations research*.
25 2007 Sep 1;153(1):29-46..
26
27 9. ESPRIT Project, 2019. URL: <http://www.esprit-transport-system.eu/> [accessed November 23, 2020]
28
29 10. Fagnant DJ, Kockelman KM. The travel and environmental implications of shared autonomous
30 vehicles, using agent-based model scenarios. *Transportation Research Part C: Emerging Technologies*.
31 2014 Mar 1;40:1-3.
32
33 11. François C, Gondran N, Nicolas JP, Parsons D. Environmental assessment of urban mobility:
34 combining life cycle assessment with land-use and transport interaction modelling—application to Lyon
35 (France). *Ecological Indicators*. 2017 Jan 1;72:597-604.
36
37 12. Gawron JH, Keoleian GA, De Kleine RD, Wallington TJ, Kim HC. Deep decarbonization from
38 electrified autonomous taxi fleets: Life cycle assessment and case study in Austin, TX. *Transportation*
39 *Research Part D: Transport and Environment*. 2019 Aug 1;73:130-41.
40
41 13. Goyal P, Ferrara E. Graph embedding techniques, applications, and performance: A survey.
42 *Knowledge-Based Systems*. 2018 Jul 1;151:78-94.
43
44 14. Grover A, Leskovec J. node2vec: Scalable feature learning for networks. In *Proceedings of the 22nd*
45 *ACM SIGKDD international conference on Knowledge discovery and data mining* 2016 Aug 13 (pp.
46 855-864).
47
48 15. Gschwind T, Irnich S. Effective handling of dynamic time windows and its application to solving the
49 dial-a-ride problem. *Transportation Science*. 2015 May;49(2):335-54.
50

- 1 16. Gurumurthy KM, Kockelman KM. Analyzing the dynamic ride-sharing potential for shared
2 autonomous vehicle fleets using cellphone data from Orlando, Florida. *Computers, Environment and*
3 *Urban Systems*. 2018 Sep 1;71:177-85.
4
5 17. Ho SC, Szeto WY, Kuo YH, Leung JM, Petering M, Tou TW. A survey of dial-a-ride problems:
6 Literature review and recent developments. *Transportation Research Part B: Methodological*. 2018 May
7 1;111:395-421.
8
9 18. Hyland MF, Mahmassani HS. Taxonomy of shared autonomous vehicle fleet management problems
10 to inform future transportation mobility. *Transportation Research Record*. 2017;2653(1):26-34.
11
12 19. Organisation for Economic Co-operation and Development. *Urban mobility system upgrade: How*
13 *shared self-driving cars could change city traffic*. OECD Publishing; 2015.
14
15 20. Jaguar Land Rover. Article titled “Jaguar Land Rover reveals Project Vector autonomous ride-share
16 vehicle”, by Alistair Charlton, 2020 Feb 19. URL: [https://www.gearbrain.com/jaguar-land-rover-project-](https://www.gearbrain.com/jaguar-land-rover-project-vector-2645188684.html)
17 [vector-2645188684.html](https://www.gearbrain.com/jaguar-land-rover-project-vector-2645188684.html) [accessed July 20, 2020].
18
19 21. Jaw JJ, Odoni AR, Psaraftis HN, Wilson NH. A heuristic algorithm for the multi-vehicle advance
20 request dial-a-ride problem with time windows. *Transportation Research Part B: Methodological*. 1986
21 Jun 1;20(3):243-57.
22
23 22. Levin MW. Congestion-aware system optimal route choice for shared autonomous vehicles.
24 *Transportation Research Part C: Emerging Technologies*. 2017 Sep 1;82:229-47.
25
26 23. Liang X, de Almeida Correia GH, Van Arem B. Optimizing the service area and trip selection of an
27 electric automated taxi system used for the last mile of train trips. *Transportation Research Part E:*
28 *Logistics and Transportation Review*. 2016 Sep 1;93:115-29.
29
30 24. Ma J, Li X, Zhou F, Hao W. Designing optimal autonomous vehicle sharing and reservation systems:
31 A linear programming approach. *Transportation Research Part C: Emerging Technologies*. 2017 Nov
32 1;84:124-41.
33
34 25. Masmoudi MA, Hosny M, Braekers K, Dammak A. Three effective metaheuristics to solve the multi-
35 depot multi-trip heterogeneous dial-a-ride problem. *Transportation Research Part E: Logistics and*
36 *Transportation Review*. 2016 Dec 1;96:60-80.
37
38 26. McNally MG. *The four-step model*. Emerald Group Publishing Limited; 2007 Sep 14.
39
40 27. Métropole de Lyon. Vallée de la Chimie Presentation, 2020. URL:
41 <https://lyonvalleedelachimie.fr/en/home/> [accessed July 27, 2020].
42
43 28. Mourad A, Puchinger J, Chu C. A survey of models and algorithms for optimizing shared mobility.
44 *Transportation Research Part B: Methodological*. 2019 May 1;123:323-46.
45
46 29. Molenbruch Y, Braekers K, Caris A. Typology and literature review for dial-a-ride problems. *Annals*
47 *of Operations Research*. 2017 Dec 1;259(1-2):295-325.
48
49 30. Narayanan S, Chaniotakis E, Antoniou C. Shared autonomous vehicle services: A comprehensive
50 review. *Transportation Research Part C: Emerging Technologies*. 2020 Feb 1;111:255-93.
51

- 1 31. Pinto HK, Hyland MF, Mahmassani HS, Verbas IÖ. Joint design of multimodal transit networks and
2 shared autonomous mobility fleets. *Transportation Research Part C: Emerging Technologies*. 2019 Jun
3 22.
4
- 5 32. Perozzi B, Al-Rfou R, Skiena S. Deepwalk: Online learning of social representations. In *Proceedings*
6 *of the 20th ACM SIGKDD international conference on Knowledge discovery and data mining* 2014 Aug
7 24 (pp. 701-710).
8
- 9 33. Psaraftis HN. A dynamic programming solution to the single vehicle many-to-many immediate
10 request dial-a-ride problem. *Transportation Science*. 1980 May;14(2):130-54.
11
- 12 34. Ropke S, Cordeau JF, Laporte G. Models and branch-and-cut algorithms for pickup and delivery
13 problems with time windows. *Networks: An International Journal*. 2007 Jul;49(4):258-72.
14
- 15 35. Sinha KC. Sustainability and urban public transportation. *Journal of Transportation Engineering*. 2003
16 Jul;129(4):331-41.
17
- 18 36. Shaheen S, Chan N. Mobility and the sharing economy: Potential to facilitate the first-and last-mile
19 public transit connections. *Built Environment*. 2016 Dec 1;42(4):573-88.
20
- 21 37. Shen Y, Zhang H, Zhao J. Integrating shared autonomous vehicle in public transportation system: A
22 supply-side simulation of the first-mile service in Singapore. *Transportation Research Part A: Policy and*
23 *Practice*. 2018 Jul 1;113:125-36.
24
- 25 38. Tang J, Qu M, Wang M, Zhang M, Yan J, Mei Q. Line: Large-scale information network embedding.
26 In *Proceedings of the 24th international conference on world wide web* 2015 May 18 (pp. 1067-1077).
27
- 28 39. TCL, Transport à la demande, 2020. URL: [https://www.tcl.fr/transport-a-la-demande-vallee-de-la-](https://www.tcl.fr/transport-a-la-demande-vallee-de-la-chimie)
29 [chimie](https://www.tcl.fr/transport-a-la-demande-vallee-de-la-chimie) (in french) [accessed July 27, 2020].
30
- 31 40. Vosooghi R, Puchinger J, Bischoff J, Jankovic M, Vouillon A. Shared autonomous electric vehicle
32 service performance: Assessing the impact of charging infrastructure. *Transportation Research Part D:*
33 *Transport and Environment*. 2020 Apr 1;81:102283.
34
- 35 41. Waymo. Article titled “*Autonomous ridesharing isn’t dead: How Waymo is adapting to the post-*
36 *COVID era*” by Ronan Glon, 2020, July 3. URL: [https://www.digitaltrends.com/cars/waymo-in-post-](https://www.digitaltrends.com/cars/waymo-in-post-covid-era/)
37 [covid-era/](https://www.digitaltrends.com/cars/waymo-in-post-covid-era/) [accessed July 20, 2020].
38